ALMA Memo 602

Atacama
Large
Millimeter
Array

ALMA Sensitivity Metric for Science Sustainability Projects

ALMA-35.00.101.666-A-SPE

2017–01–23

Description Document

Jeff Mangum (NRAO)

Change Record

Revision	Date	Author	Section/ Page affected	Remarks
1	2016-09-14	Jeff Mangum	All	Initial draft
2	2016-10-03	Jeff Mangum	All	Modifications based on feedback
3	2016-10-09	Jeff Mangum	All	Modifications based on feedback
4	2016-11-08	Jeff Mangum	All	Modifications to T_{rx} table values
4	2016-11-09	Jeff Mangum	§2,Table 3	Updated Bands 4, 8, and 10 T_{rx}
5	2017-01-15	Jeff Mangum	All	Updates based on Carpenter comments
6	2017-01-23	Jeff Mangum	2,3	Clarification of correlator efficiencies

Contents

1 Summary

This document proposes a standard metric for comparing the relative merits of Science Sustainability Projects under consideration.

2 Tradeoff Analysis

Using the radiometer equation (Equation 3) one can derive "tradeoff" equations which compare improved performance in $\sigma_{radiometer}$, T_{sys}, η_c, f_N, $\Delta\nu$, and t_{int}:

$$\frac{\sigma_{\rm radiometer}^{\rm improved}}{\sigma_{\rm radiometer}} = \left(\frac{T_{\rm sys}^{\rm improved}}{T_{\rm sys}}\right)\left(\frac{\eta_{\rm c}}{\eta_{\rm c}^{\rm improved}}\right)\sqrt{\left(\frac{f_{\rm N}}{f_{\rm N}^{\rm improved}}\right)\left(\frac{\Delta\nu}{\Delta\nu^{\rm improved}}\right)\left(\frac{t_{\rm int}}{t_{\rm int}^{\rm improved}}\right)} \quad (1)$$

$$\frac{t_{\rm int}^{\rm improved}}{t_{\rm int}} = \left[\left(\frac{\sigma_{\rm radiometer}}{\sigma_{\rm radiometer}^{\rm improved}}\right)\left(\frac{T_{\rm sys}^{\rm improved}}{T_{\rm sys}}\right)\left(\frac{\eta_{\rm c}}{\eta_{\rm c}^{\rm improved}}\right)\right]^2\left(\frac{f_{\rm N}}{f_{\rm N}^{\rm improved}}\right)\left(\frac{\Delta\nu}{\Delta\nu^{\rm improved}}\right) \quad (2)$$

with the obvious conclusion that sensitivity degrades linearly with system temperature and correlator efficiency, and degrades much slower as the square-root of the number of antennas ($f_{\rm N}$), the bandwidth ($\Delta\nu$), and the integration time (t_{int}). The following sections describe the radiometer equation and the terms used to calculate it.

Taking an example of how to use this metric, assume that one would like to consider a 10% to 20% improvement in receiver temperature for a particular ALMA receiver band. One can use Equation 1 to calculate what the improvement in RMS would be for such an upgrade by setting $T_{\rm rx}^{\rm improved}$ equal to the receiver band's upgraded receiver temperature and $T_{\rm rx}$ equal to the current receiver temperature in Equation 6. For a fixed integration time ($t_{int} = t_{int}^{improved}$), the resulting system temperature ratio, $\frac{T_{\rm sys}^{\rm improved}}{T_{\rm sys}}$, is shown in Figure 1 for two representative ALMA atmospheric opacity octiles. From these calculations we see that a 10% improvement in T_{rx} for Band 6 results in a 7%/6% improvement in $\sigma_{radiometer}$ for first/fourth octile atmospheric opacity conditions. This improvement in T_{rx} translates to a $(1.07^2)/(1.06^2) = 14.5\%/12.4\%$ decrease in the amount of integration time required to reach a given sensitivity (Equation 2).

Taking another example, one of the ALMA baseline correlator upgrade proposals includes an upgrade from 3- to 4-bit sampling, which represents an improvement in the quantization efficiency η_q from 96% to 99% for many correlator modes. This would translate to an $\left(\frac{0.99}{0.96}\right)^2 =$ 6% decrease in the amount of integration time required to reach a given sensitivity.

As actual instrumentation upgrades often involve multiple improvements, Table 1 lists two study and/or development projects currently funded through the ALMA North American or European development (science sustainability) programs. Each upgrade involves improvements

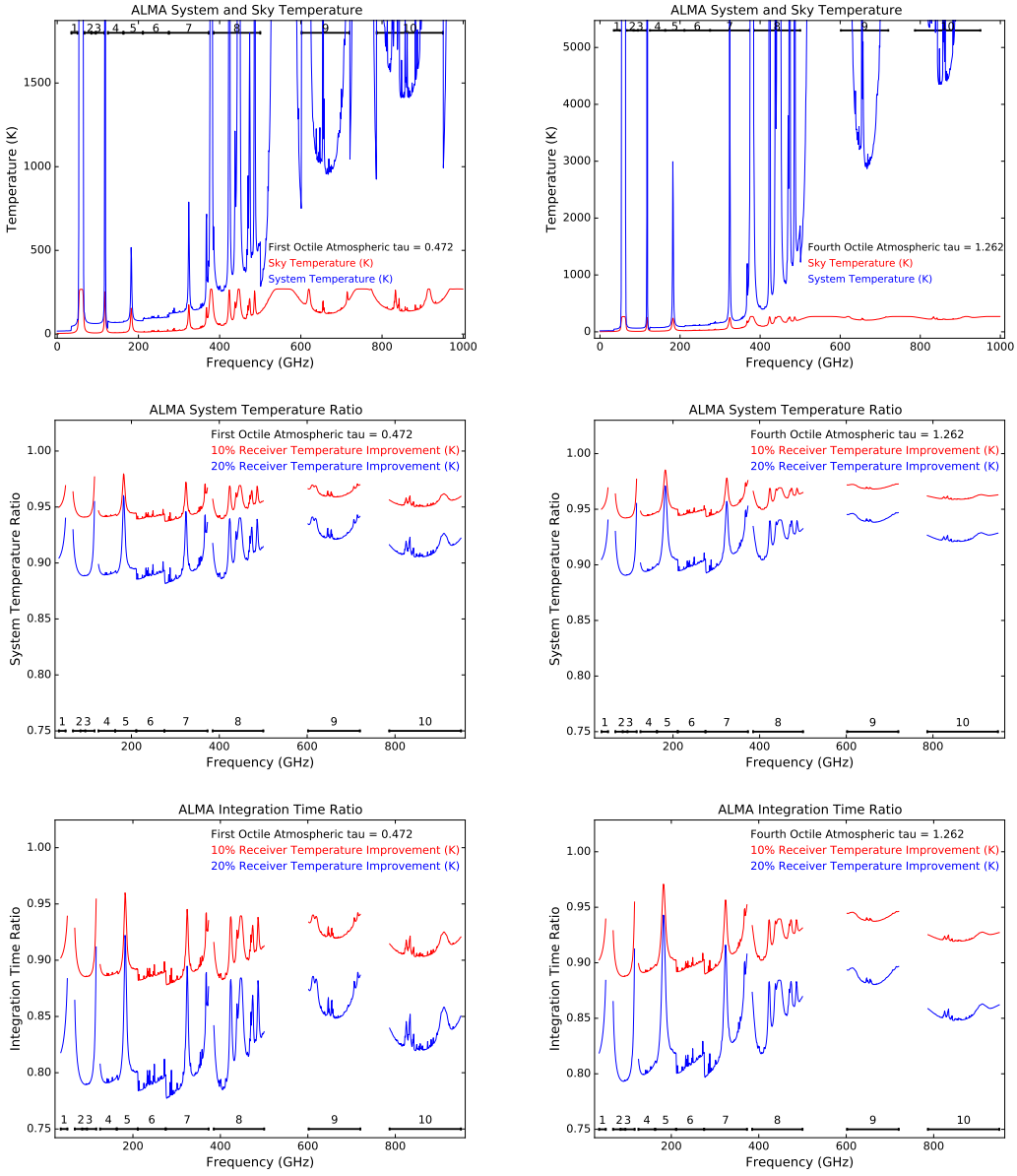

Figure 1: ALMA system and sky temperature (top), system temperature ratio (middle), and integration time ratio (bottom) for first octile (left; best 12.5%) and fourth octile (right; best 50%) atmospheric opacity conditions on the ALMA site. The T_{sys} calculations are derived from the CASA implementation of Juan Pardo's ATM atmospheric model (using Todd Hunter's au:plotAtmosphere with a new option to export model calculations to a file; Pardo, 2001), and assume $T_{amb} = 270\,K$, $\eta_{eff} = 0.95$, and appropriate sideband gain for each receiver band.

in one or more of the terms listed in Equations 1 or 2. The last two columns in Table 1 list the resultant maximum improvements in $\sigma_{radiometer}$ and t_{int} for each upgrade.

Table 1: ALMA Upgrades and Sensitivity

Upgrade	Improved/Current Ratio					
	T_{rx}	T^a_{sys}	η_c	$\Delta\nu$	$\sigma_{radiometer}$	t_{int}
Band 6	0.9	0.94	1.0	1.6[b]	0.74	0.55
Band 10	0.5	0.66[c]	1.0	1.0	0.66	0.44
Correlator	1.0	1.0	0.97	1.0	0.97	0.94

[a] Assuming first-octile weather conditions.
[b] Bandwidth expansion from 5–10 to 4–12 GHz. Direct improvement to continuum sensitivity.
[c] Note that the Band 10 upgrade includes a change from DSB to 2SB in addition to an improvement by approximately a factor of 2 in T_{rx}.

3 The Radiometer Equation

Drawing heavily from Chapter 9 of the ALMA Technical Handbook (ALMA Partnership, 2016) and Mangum (2015), the point-source sensitivity given a requested amount of on-source observing time can be estimated using the formalism. The sensitivity to a point-source from an interferometer or single antenna (total power), $\sigma_{\rm radiometer}$, is given by:

$$\sigma_{\rm radiometer} = \frac{w_r\, 2\, k\, T_{\rm sys}}{\eta_{\rm q}\eta_{\rm c}\eta_{\rm A} A_{\rm g}(1-f_s)\sqrt{f_N\, n_{\rm p}\, \Delta\nu\, t_{\rm int}}}. \quad (3)$$

where

- w_r – robust weighting factor. Pipeline imaging and subsequent QA2 assessment is performed assuming that the visibilities are weighted using robust weighting, specifically a Briggs robustness factor of 0.5. Simulations have shown that w_r is equal to 1.1 for a Briggs robustness value of 0.5. For total power measurements $w_r = 1$.
- $T_{\rm sys}$ – System temperature. See Equation 6.
- $\eta_{\rm q}$ – quantization efficiency. A fundamental limit on the achievable sensitivity is set by the initial sampler digitization of the baseband signals. This is equal to 0.96 and 0.99 for 3-bit and 4-bit sampling, respectively.

- η_c – correlator efficiency. This depends on the correlator (64-input or ACA) and correlator mode, although the efficiency of all implemented 64-input correlator modes is equal to 0.88[1]. The ACA efficiencies *do* depend on the mode.
- η_A – aperture efficiency. See Section 3.6 and Equation 14 for details. Table 4 lists values for ALMA antenna efficiencies in various ALMA bands.
- A_g – geometric area of the antenna. See Section 3.6.
- f_s – shadowing fraction. For the more compact 12-m configurations and the ACA 7-m array, antennas can block the field-of-view of other antennas in the array and thus reduce the total collecting area. The shadowing fraction is a function of source declination as shown in Section 7 of ALMA Partnership (2016). For total power measurements $f_s = 0$.
- f_N – antenna number factor. $f_N = N\,(N-1)$ for interferometer measurements, while $f_N = N$ for total power measurements.
- n_p – number of polarizations. $n_p = 1$ for single polarization and $n_p = 2$ for dual and full polarization observations
- $\Delta\nu$ – spectral resolution element width. This is 7.5 GHz for continuum observations, and to the spectral resolution for spectral line measurements.
- t_{int} – total on-source integration time for an interferometer, or total on-source t_{on} and off-source t_{off} integration time, with $t_{on} = t_{off}$, for total power measurements.

The associated surface brightness sensitivity (K) is related to the point-source sensitivity (Jy) by

$$\sigma_T = \frac{\sigma_{\rm radiometer}\lambda^2}{2k\ \Omega} \tag{4}$$

where Ω is the beam solid angle. This is related to the user-entered spatial resolution, θ, by

$$\Omega = \frac{\pi\theta^2}{4\ln 2}. \tag{5}$$

This assumes that the telescope beam is a circular Gaussian with a half power beamwidth of θ.

[1]There are hardware-implemented 64-input correlator modes that have efficiecies of 0.94 (double Nyquist), 0.99 (4-bit Nyquist and double Nyquist), and 1.00 (3-bit TDM Nyquist) (Escoffier *et al.*, 2008). These correlator modes have not yet been implemented in the acquisition software.

3.1 System Temperature

The system temperature is given by:

$$T_{\rm sys} = \frac{1}{\eta_{\rm eff} e^{-\tau_0 \sec z}} \left[(1+g) \times \left(T_{\rm rx} + \frac{h\nu}{2k} \right) + \eta_{\rm eff} \left(T_{\rm sky,s} + g T_{\rm sky,i} \right) + (1 - \eta_{\rm eff}) \times \left(T_{\rm amb,s} + g T_{\rm amb,i} \right) \right] \tag{6}$$

where

- g – sideband gain ratio. Equal to 0 for SSB and 2SB receivers, and 1 for DSB receivers.
- $T_{\rm rx} + \frac{h\nu}{2k}$ – receiver temperature with half-photon zero-point fluctuation correction[2]
- $T_{\rm sky,s}$ – sky temperature at the requested frequency in the signal sideband
- $T_{\rm sky,i}$ – sky temperature in the image sideband
- $T_{\rm amb,s}$ – ambient temperature in the signal sideband
- $T_{\rm amb,i}$ – ambient temperature in the image sideband
- $\eta_{\rm eff}$ – the coupling factor, or forward efficiency. This is equal to the fraction of the antenna power pattern that is contained within the main beam and is currently fixed at 0.95
- $e^{-\tau_0 \sec z}$ – the fractional transmission of the atmosphere, where τ_0 is equal to the zenith atmospheric opacity and $\sec z$ is the airmass at transit.

The terms $\eta_{\rm eff}$ and $e^{-\tau_0 \sec z}$ both attenuate the source signal and we thus divide through by them in order to obtain a measure of the system noise that is relative to the unattenuated source. Note that this is always done at the *signal* frequency.

3.2 Sky Temperature

The atmospheric zenith opacity, τ_0, and the sky temperature, $T_{\rm sky}$, can be calculated using a model of the atmospheric emission and absorption. ALMA uses the Atmospheric Transmission at Microwaves (ATM) model (Pardo, 2001). For ALMA this model calculates the sky temperature by integrating the atmospheric temperature profile, this having been formed from the average of 28 radiosonde measurements taken at the ALMA site during November 1999. The

[2]We believe that there might be an error in the current version of the ALMA Technical Handbook regarding the contribution of the zero-point (vacuum) fluctuations to the overall system temperature. According to Tony Kerr, this term ($\frac{h\nu}{2k}$) is normally not applied to the receiver temperatures quoted by receiver builders, and it is not normally considered part of the source (sky + atmosphere) temperature, so it must be included elsewhere in the system temperature calculation. In Equation 6, it is included explicitly with T_{rx}.

model output provides values of the atmospheric opacity and "output radiance", in steps of 100 MHz, for the seven different octiles of PWV (Table 2). The sky temperature is converted from the radiance using the Planck function and includes the contribution due to the CMB.

The ATM code only provides measurements of the sky temperature at the zenith, $T_{\rm sky}(z = 0)$, and therefore one must account for the greater atmospheric emission at lower elevations. Normally one does this zenith angle correction by assuming that the emission from the atmosphere can be approximated as

$$T_{\rm sky} = T_{\rm atm}(1 - e^{-\tau_0 \sec z}). \tag{7}$$

Inserting the ATM values of $T_{\rm sky}(z = 0)$ and τ_0 into Equation 7 allows the mean physical temperature of the atmosphere, $T_{\rm atm}$, to be measured i.e.

$$T_{\rm atm} = \frac{T_{\rm sky}(z = 0)}{(1 - e^{-\tau_0})}. \tag{8}$$

This can be reinserted into Equation 7 to calculate the sky temperature at any zenith angle as

$$T_{\rm sky}(z) = T_{\rm sky}(z = 0)\frac{(1 - e^{-\tau_0 \sec z})}{(1 - e^{-\tau_0})} \tag{9}$$

$T_{\rm sky}(z)$ then need to be corrected for the fact that the required noise temperatures ($T_{\rm n}$) are defined assuming $P_\nu = kT$ and thus a correction for the Planck law is required, i.e.

$$T_{\rm n} = T \times \left(\frac{h\nu/kT}{e^{h\nu/kT} - 1}\right) \tag{10}$$

3.3 CMB Temperature

The temperature of the Cosmic Microwave Background is included in $T_{\rm sky}$.

3.4 Receiver Temperatures

Table 3 lists the assumed receiver temperatures for all ALMA bands, which include on-array measurements for Bands 3 through 10 (Phillips, 2016). For ALMA Bands 3, 6, 7, 8 and 9, typical values measured in the laboratory are consistent with the on-array measurements (references given in the footnotes to Table 3). The measured values are somewhat conservative and so are in between what we might expect at the middle and edges of the bands. Note that single sideband noise temperatures are reported for Bands 1-8 and double sideband temperatures for Bands 9 and 10.

Octile	PWV (mm)
1	0.472
2	0.658
3	0.913
4	1.262
5	1.796
6	2.748
7	5.186

Table 2: Octiles of PWV measured at the ALMA site from years of monitoring data. The first octile corresponds to the best weather conditions and shows that 12.5% of the time, PWV values at least as good as 0.472 mm can be expected. Subsequent octiles give the corresponding value for 25%, 37.5%. etc.

The receiver noise temperatures quoted by receiver builders are normally deduced from Y-factor measurements using hot and cold loads. The noise temperatures of the hot and cold loads are usually derived from their physical temperature either assuming the Rayleigh-Jeans law ($T_n = T_{physical}$), or via the Callen and Welton formula:

$$T_n = T_{physical}\left[\frac{\frac{h\nu}{kT_{physical}}}{\exp\left(\frac{h\nu}{kT_{physical}}\right)-1}\right] + \frac{h\nu}{2k}, \tag{11}$$

which differs from the Rayleigh-Jeans value by much less than $\frac{h\nu}{2k}$ in the range of frequencies and temperatures concerned. For example, at 100 GHz $\frac{h\nu}{2k} = 2.4$ K, and for a 77 K cold load the Rayleigh-Jeans and Callen and Welton noise temperatures differ by only 0.025 K which is smaller than the uncertainty in the receiver noise measurement. A detailed explanation is given in Kerr & Randa (2010).

3.5 Ambient Temperature

This is essentially spillover from the sidelobes of the antenna beam corresponding to emission from the ground and the telescope itself. A reasonable assumption is to hold this parameter constant at 270 K (median value as measured from many years of monitoring data at the ALMA site). One must convert the ambient temperature to a noise temperature according to Equation 10 and thus its total contribution is frequency dependent and can vary between the different sidebands.

ALMA Band	Receiver Type	$T_{\rm rx,spec}$ (K)	$T_{\rm rx,assumed}$ (K)
1	SSB	17	23[a]
2	SSB	30	37[b,c]
3	2SB	37	37[c,d]
4	2SB	51	40[c,e]
5	2SB	65	35[c,f]
6	2SB	83	40[c]
7	2SB	147	65[c]
8	2SB	196	115[e,g]
9	DSB	175	95[g]
10	DSB	230	180[e,g]

[a] Measured values from Huang *et al.* (2016).
[b] Lab measurements from Pospieszalski (private communication).
[c] From on-array measurements (Phillips, 2016).
[d] Lab measurements from Saini (private communication).
[e] From Daisuke (private communication).
[f] Based on measurements of first 32 receivers.
[g] On-array measured values vary from 70–120 K, 65–120 K, and 175–275 K for 390–495 GHz, 610–710 GHz, and 795–940 GHz, respectively (Phillips, 2016).

Table 3: Receiver temperatures (and their specifications) as a function of ALMA band. For most of the bands we are currently assuming the ALMA specification for the receiver temperature that should be achieved across 80% of the band, $T_{\rm rx,spec}$. Updates to the measured values for $T_{\rm rx,assumed}$ quoted in the ALMA Technical Handbook are provided with references.

3.6 Aperture Efficiency

From Mangum (2015) the aperture efficiency η_A is defined as follows:

$$\eta_A \equiv \frac{A_{max}}{A_g} \tag{12}$$

where

- A_{max} is the maximum area of the antenna that can effectively collect photons
- A_g is the geometrical area of the antenna ($\frac{\pi d^2}{4}$). For the ALMA 12 m and 7 m antennas $A_g = 113.1\,m^2$ and $38.5\,m^2$, respectively.

The aperture efficiency defines the efficiency with which the radiation from a point source is collected by an antenna. As the aperture efficiency is determined by the product of a number of efficiencies, it is often convenient to calculate η_A from these individual efficiency terms:

$$\eta_A \equiv \eta_i \eta_s \eta_r \eta_p \eta_e \eta_f \eta_b \tag{13}$$

Mangum (2015) defines the individual component efficiencies that form the aperture efficiency. For the ALMA antennas the aperature efficiency can be written as follows:

$$\begin{aligned}\eta_A &= \frac{3\left(1+\tau\right)^2 \eta_s \eta_b \eta_r \eta_p \eta_f}{4\left(1+\tau+\tau^2\right)} \left\{ \exp\left[-\left(\frac{4\pi\sigma}{\lambda}\right)^2 \right] + \frac{1}{\eta_{A0}} \left(\frac{c}{D}\right)^2 \left\{ 1 - \exp\left[-\left(\frac{4\pi\sigma}{\lambda}\right)^2 \right] \right\} \right\} \\ &\simeq \eta_s \eta_r \eta_p \eta_f \frac{3\left(1+\tau\right)^2}{4\left(1+\tau+\tau^2\right)} \exp\left[-\left(\frac{4\pi\sigma}{\lambda}\right)^2 \right]\end{aligned} \tag{14}$$

where $\log(\tau) = T_e/20$ (beam taper T_e in dB) and we assume that the correlation length of the surface errors are small in comparison to the diameter of the antenna ($c \ll D$). Therefore, for the following conditions:

- For a feed taper of $T_e = -15.13\,\mathrm{dB}$ (appropriate for 100 GHz derived from the TICRA models of the Vertex antennas; see Todd Hunter's theoretical beam shape analysis at `https://safe.nrao.edu/wiki/bin/view/Main/ALMABeamsVsTheoretical`),
- A surface accuracy of $\sigma = 25\,\mu$m,
- A blockage efficiency of $\eta_b = 0.94$,
- A spillover efficiency of $\eta_s = 0.95$,

- A polarization efficiency of $\eta_p = 0.99$,
- Radiation and focus efficiency = 1,

we calculate $\eta_A \simeq 0.75$ at 100 GHz for the ALMA DV and DA 12 m antennas. Figure 2 shows the aperture efficiency (Equation 14) for $\sigma = 25\,\mu$m (appropriate for the 12 m antennas) and 20μm (appropriate for the 7 m antennas).

Table 4: ALMA Antenna Standard Continuum Band Efficiencies

Band	Frequencies (GHz)	Beam Taper[a] (dB)	η_A^b	SEFD[b] (Jy/K)
3	91.5	15.13	0.75/0.75	32.45/95.04
3	103.5	15.13	0.75/0.75	32.53/95.20
4	139.0	10.30	0.79/0.80	30.87/90.03
4	151.0	10.30	0.79/0.79	30.99/90.25
6	225.0	10.84	0.76/0.77	32.18/92.70
6	241.0	9.34	0.77/0.78	31.80/91.34
7	337.5	11.50	0.70/0.73	34.80/97.77
7	349.5	11.72	0.69/0.73	35.22/98.63
8	399.0	11.50	0.67/0.71	36.58/100.94
8	411.0	11.72	0.65/0.70	37.08/101.92
9	677.0	10.93	0.48/0.58	50.42/123.61
9	681.0	10.93	0.48/0.58	50.72/124.08
10	873.0	10.93	0.35/0.47	70.38/153.03
10	877.0	10.93	0.34/0.47	70.92/153.78

Assuming $\eta_b = 0.94$, $\eta_s = 0.95$, $\eta_p = 0.99$, $\eta_r = 1.0$, and $\eta_f = 1.0$.
[a] From Todd Hunter's TICRA beam analysis.
[b] 12 m / 7 m assuming $\sigma = 25/20\mu$m.

References

ALMA Partnership, 2016, S. Asayama, A. Biggs, I. de Gregorio, W. Dent, J. Di Francesco, E. Fomalont, A. Hales, E. Humphries, S. Kameno, E. Muller, B. Vila Vilaro, E. Villard, F. Stoehr (ISBN 978-3-923524-66-2)

Escoffier, R., Webber, J., & Baudry, A. 2008, "64 Antenna Correlator Specifications and Requirements", ALMA-60.00.00.00-001-C-SPE

Huang, Y. D., Morata, O., Koch, P. M., *et al.*, 2016, Proc. SPIE, 9911

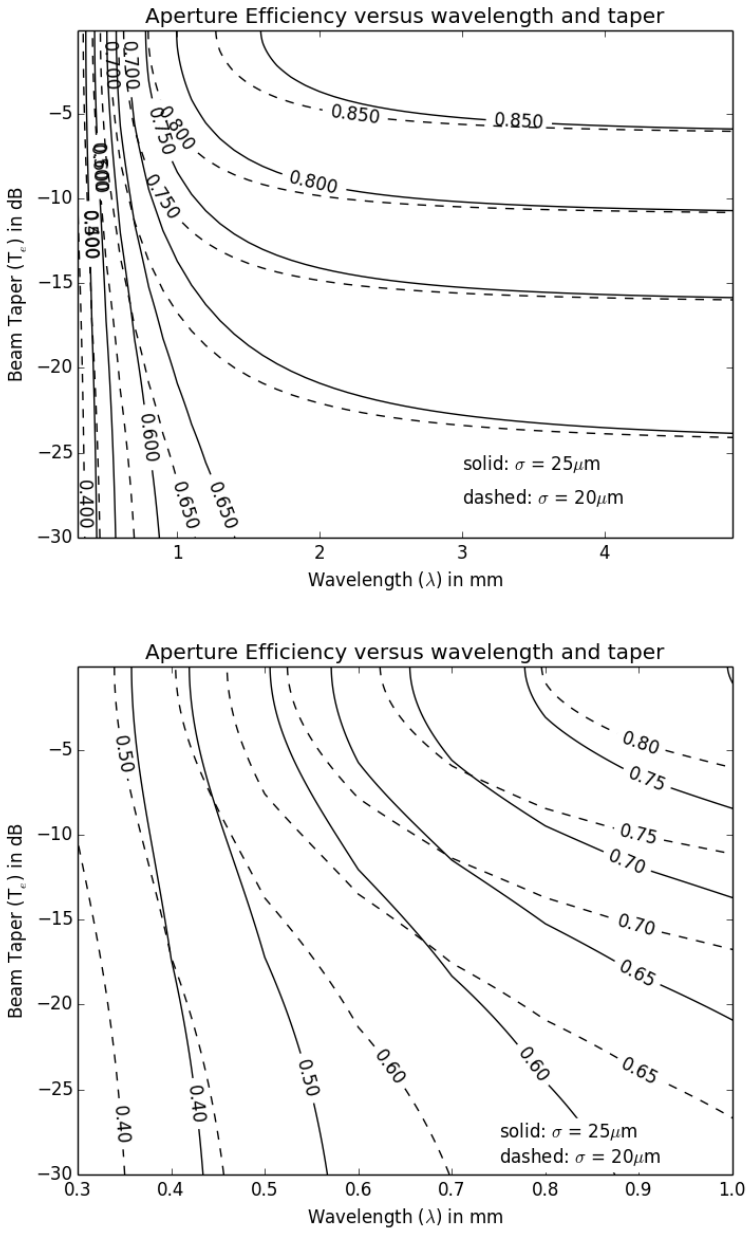

Figure 2: Aperture efficiency (η_A; Equation 14) as a function of the observing wavelength (in mm, top for $\lambda = 0.3$ to 4 mm and bottom for $\lambda = 0.3$ to 1 mm) and beam taper (in dB) for a blockage efficiency $\eta_b = 0.94$, spillover efficiency $\eta_s = 0.95$, polarization efficiency $\eta_p = 0.99$, radiation efficiency $\eta_r = 1.0$, and focus efficiency $\eta_f = 1.0$. The surface accuracy is assumed to be $\sigma = 25\,\mu$m (solid contours) for the 12 m antennas and 20 μm (dashed contours) for the 7 m antennas. Note how for $\lambda \gtrsim 2$ mm the illumination efficiency η_i dominates, but at $\lambda \lesssim 2$ mm the surface efficiency η_e dominates the calculation.

Kerr, A. R. & Randa, J., "Thermal Noise and Noise Measurements a 2010 Update," IEEE Microwave Magazine, vol. 11, no. 6, pp. 40-52, Oct. 2010. `http://ieeexplore.ieee.org/stamp/stamp.jsp?tp=&arnumber=5564380`

Mangum, J. G. 2015, "ALMA Antenna Efficiency", ALMA-35.00.101.666-A-SPE, 2015-03-07

Pardo, J. R., Cernicharo, J., Serabyn, E., 2001, ITAP, 49, 1683

Phillips, N. 2016, private communication